J Solid State Electrochem (2012) 16:205–211
DOI 10.1007/s10008-011-1305-z

ORIGINAL PAPER

Effect of Nb-doping on electrochemical stability of $Li_4Ti_5O_{12}$ discharged to 0 V

Bingbing Tian · Hongfa Xiang · Le Zhang · Haihui Wang

Received: 5 November 2010 / Revised: 1 January 2011 / Accepted: 7 January 2011 / Published online: 3 February 2011

Abstract $Li_4Ti_{4.95}Nb_{0.05}O_{12}$ is synthesized by a citric acid-assistant sol–gel method. X-ray diffraction (XRD) reveals that highly crystalline $Li_4Ti_{4.95}Nb_{0.05}O_{12}$ without any impurity is obtained. The electrochemical performances of the $Li_4Ti_{4.95}Nb_{0.05}O_{12}$ and the $Li_4Ti_5O_{12}$ in the range from 0 to 2.5 V are investigated. The $Li_4Ti_{4.95}Nb_{0.05}O_{12}$ presents a higher specific capacity and better cycling stability than the $Li_4Ti_5O_{12}$ due to the improved conductivity. The $Li_4Ti_{4.95}Nb_{0.05}O_{12}$ exhibits a capacity as high as 231.2 mAh g^{-1} after 100 cycles, which is much higher than the $Li_4Ti_5O_{12}$ (111.1 mAh g^{-1}). The effect of Nb-doping on electrochemical performance of $Li_4Ti_5O_{12}$ discharged to 0 V has also been discussed.

Keywords Lithium-ion batteries · $Li_4Ti_{4.95}Nb_{0.05}O_{12}$ · $Li_4Ti_5O_{12}$ · Anode materials

Introduction

Spinel $Li_4Ti_5O_{12}$ has been attracted more attention as a promising anode material for lithium-ion batteries [1–6]. It has many advantages compared to the currently used graphite, such as an excellent lithium-ion insertion/extraction reversibility and very flat voltage plateau at around 1.55 V vs. Li^+/Li. However, $Li_4Ti_5O_{12}$ exhibits poor electronic and lithium ionic conductivities, which result in its poor electrochemical performance and prevent $Li_4Ti_5O_{12}$ from being implemented commercially. In order to improve the conductivity, three methods were proposed, including synthesis of nano-sized $Li_4Ti_5O_{12}$ particles [7–14], incorporation of good conductive phase of metal powder or carbon [15–20], substituting Li or Ti with metal ions. So far, a lot of metal ions such as Cr^{3+}, V^{5+}, Mn^{4+}, Fe^{3+}, Al^{3+}, Ga^{3+}, Co^{3+}, Cu^{2+}, and Ta^{5+} were doped into $Li_4Ti_5O_{12}$ and improved electrochemical performances were observed [21–27].

Recently, the electrochemical behaviors of $Li_4Ti_5O_{12}$ discharged to 0 V have been widely investigated [28–32]. Ge et al. [28] reported the theoretical capacity of $Li_4Ti_5O_{12}$ in the voltage range from 2.5 to 0.01 V was 293 mAh g^{-1}, which was calculated on basis of full transition from Ti^{4+} to Ti^{3+}. Xiang and his coworkers [31] disclosed that the additional capacity of $Li_4Ti_5O_{12}$ below 1 V could be used to enhance the safety characteristic of the 3 V $LiNi_{0.5}Mn_{1.5}O_4/Li_4Ti_5O_{12}$ cell when the capacity was limited by the $Li_4Ti_5O_{12}$ anode. So, it is very important to investigate the electrochemical properties and cell performances of $Li_4Ti_5O_{12}$ discharged to 0 V in order to improve the energy density and safety characteristic of the corresponding batteries. However, from Shu's [29] and Borghols' [31] reports, it can be easily found that $Li_4Ti_5O_{12}$ shows a much rapid capacity loss when discharged to 0 V with increasing the cycling number, especially at a high current rate. Borghols and his coworkers [31] reported the size effect in the $Li_{4+x}Ti_5O_{12}$ spinel and concluded that the reversible intercalation and extraction of Li^+ between $Li_4Ti_5O_{12}$ and $Li_{8.5}Ti_5O_{12}$ were affected by the size of the material. In our previous work, we developed a novel Nb-doping compound, i.e., $Li_4Ti_{4.95}Nb_{0.05}O_{12}$, which possessed better electrochemical performances than $Li_4Ti_5O_{12}$ due to the improved electronic conductivity when dis-

B. Tian · H. Xiang · L. Zhang · H. Wang (✉)
School of Chemistry & Chemical Engineering, South China University of Technology,
Wushan Road,
Guangzhou 510640, China
e-mail: hhwang@scut.edu.cn

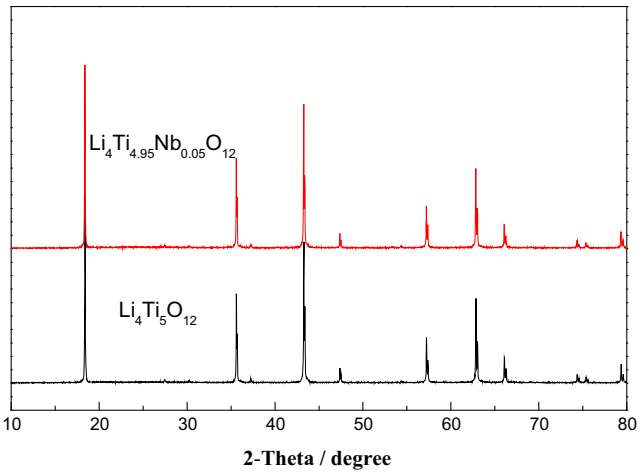

Fig. 1 XRD patterns of $Li_4Ti_5O_{12}$ and $Li_4Ti_{4.95}Nb_{0.05}O_{12}$

charged to 1 V [32]. In this paper, the effect of Nb-doping on the electrochemical performance of $Li_4Ti_5O_{12}$ discharged to 0 V was investigated.

Experimental

$Li_4Ti_{4.95}Nb_{0.05}O_{12}$ was synthesized by a sol–gel method with citric acid (AR, Sinopharm Chemical Reagent Co., Ltd., China) as a chelating agent. The stoichiometric amounts of lithium acetate (CH_3COOLi, 99%, Shanghai China Lithium Industrial Co., Ltd. China), tetrabutyl titanate ($Ti(OC_4H_9)_4$, ≥98%, Shanghai Lingfeng Chemical Reagent Co., Ltd., China) and niobium hydroxide ($Nb(OH)_5$, ≥99.5%, Guangzhou Litop Non-ferrous Metals Co., Ltd. China) were added as starting materials in ethanol to form a sol. A gel was obtained after the sol was dried at

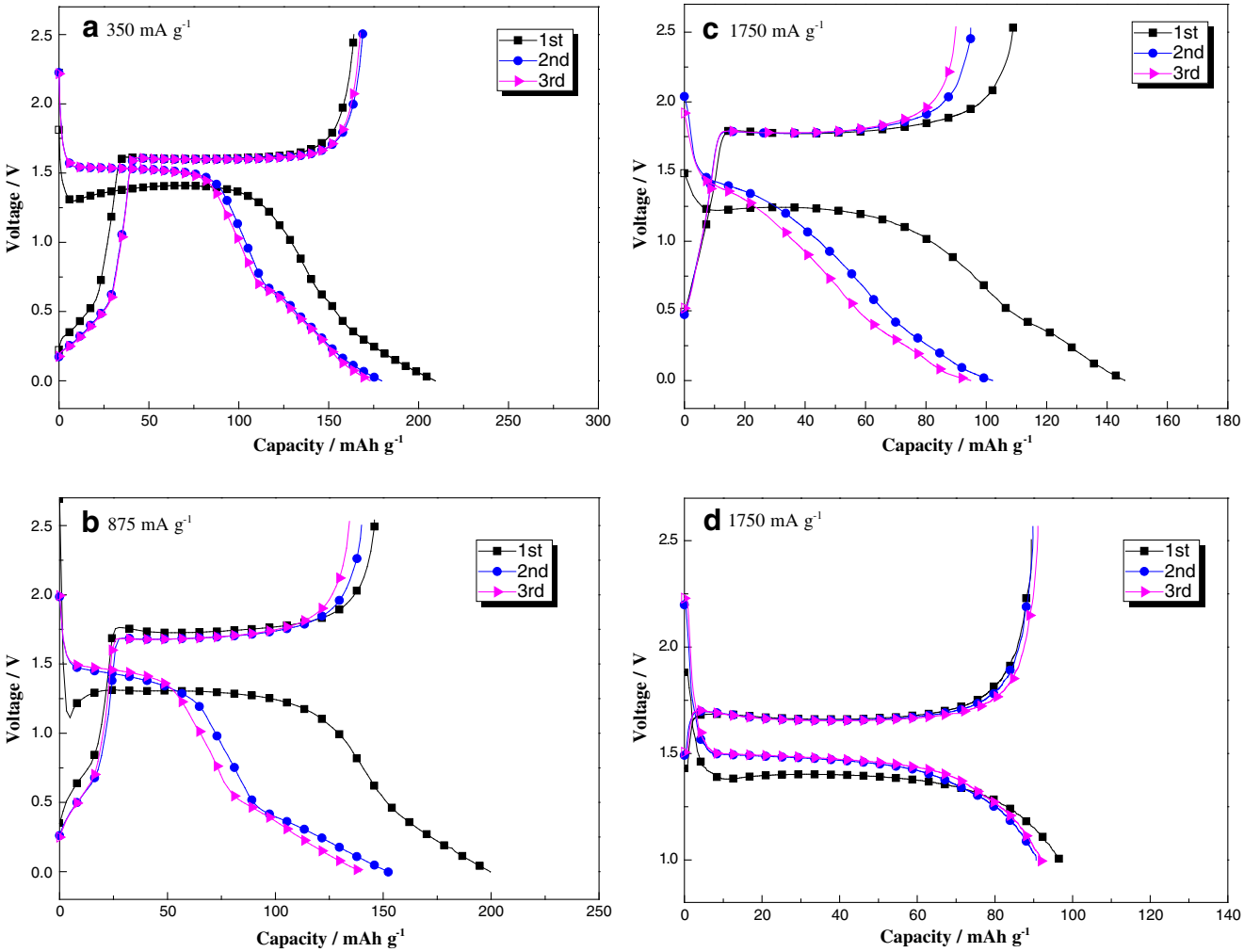

Fig. 2 The first, second, and third discharge–charge curves of the $Li_4Ti_5O_{12}$ discharged to 0 V at the current density of **a** 350 mA g^{-1}, **b** 875 mA g^{-1}, and **c** 1,750 mA g^{-1}; The first, second, and third discharge–charge curves of the $Li_4Ti_5O_{12}$ discharged to 1 V at the current density of 1,750 mA g^{-1} (**d**)

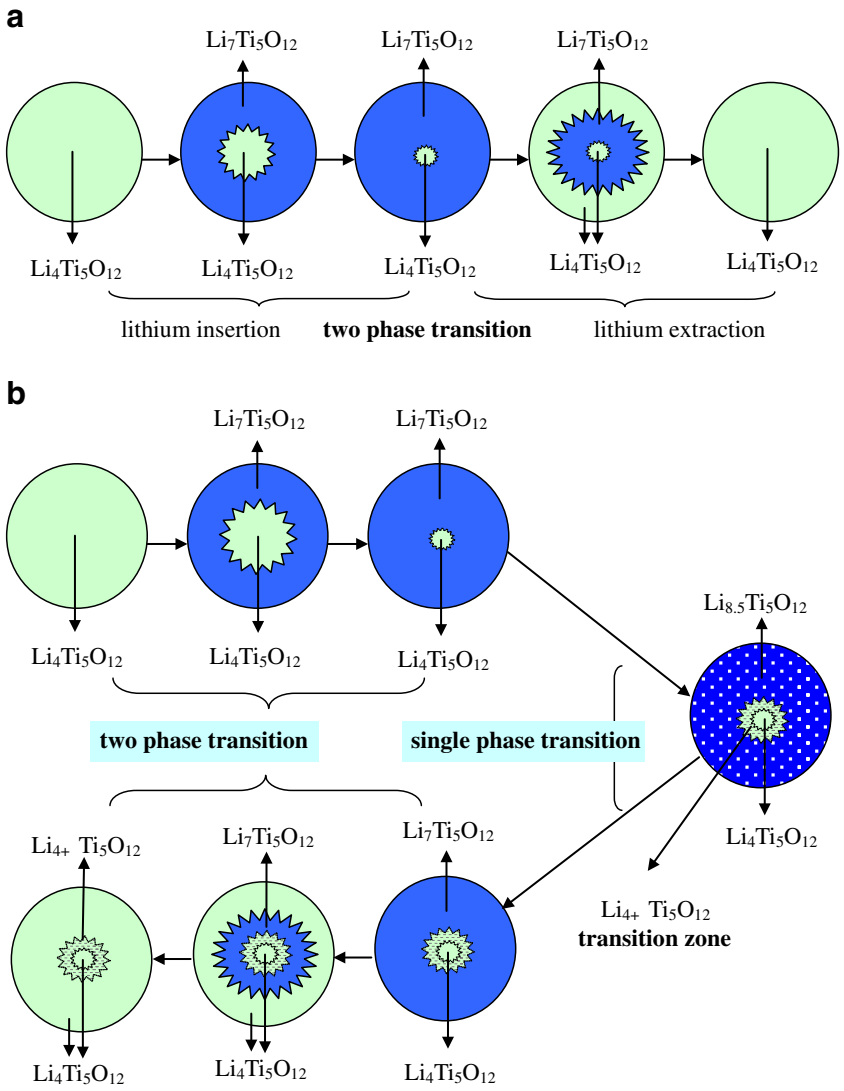

Fig. 3 Sketch map of lithium-ion intercalation and extraction for $Li_4Ti_5O_{12}$ discharge to **a** 1 V and **b** 0 V at the current density of 1,750 mA g^{-1}

80 °C to evaporate ethanol. The obtained gel was dried at 120 °C over 10 h to evaporate excess ethanol and yield organic precursor. Furthermore, the precursor was calcined in an oven at 500 °C for 2 h in air and then calcined in the oven at 850 °C for 10 h in N_2 atmosphere to obtain the final powder. The color of the powder is light blue. For comparison, the $Li_4Ti_5O_{12}$ powder was also prepared using the similar method, while the product is white. The crystal structures of the powders were characterized by X-ray diffraction (XRD, Rigaku DMax-RB) using Cu-Kα radiation ($10° \leq 2\theta \leq 80°$).

The electrochemical properties of $Li_4Ti_{4.95}Nb_{0.05}O_{12}$ and $Li_4Ti_5O_{12}$ were tested in CR2025 cells with lithium as counter electrode. A mixed solvent of ethylene carbonate (EC) and dimethyl carbonate (1:1 *w*/*w*) containing 1.0 mol dm^{-3} $LiPF_6$ was used as electrolyte and Celgard 2325 microporous membrane as separator. The electrodes contained active material, carbon black and polyvinylidene fluoride (82 : 10 : 8, by weight). The cell was assembled in an argon filled glove box (Mikrouna, super 1220), where the oxygen and moisture contents were less than 1 ppm. All the electrochemical tests were carried out at room temperature. Charge–discharge cycling tests were performed at indicated current densities using a NEWARE Battery Testing System.

Results and discussion

Figure 1 shows the XRD patterns of $Li_4Ti_5O_{12}$ and $Li_4Ti_{4.95}Nb_{0.05}O_{12}$ powders. The diffraction peaks of the powders conform to JCPDS card No. 49-0207, indicating that the synthesized powders are in accordance with the spinel $Li_4Ti_5O_{12}$ standard without any impurity detected. In

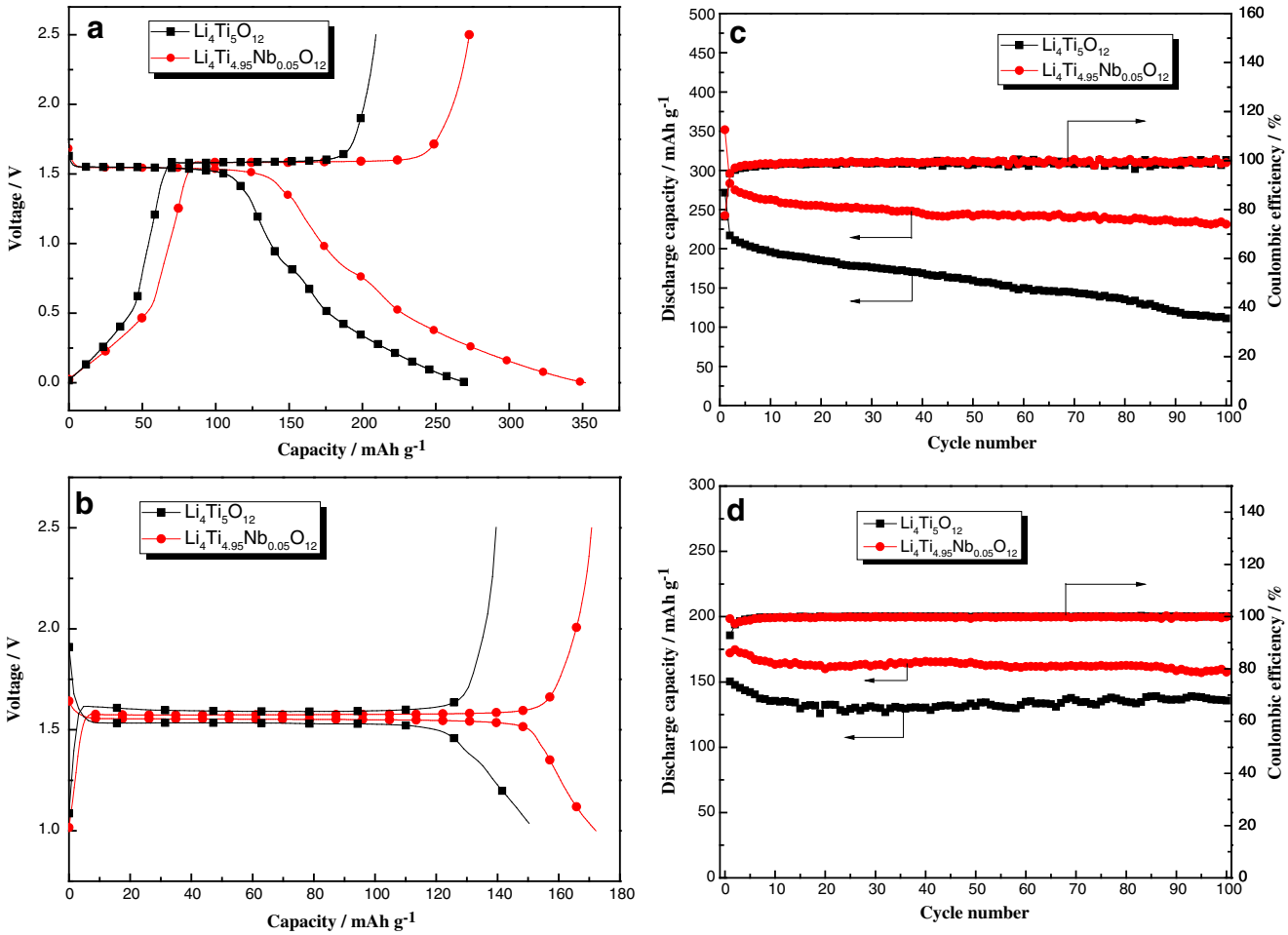

Fig. 4 Initial discharge–charge curves of $Li_4Ti_5O_{12}$ and $Li_4Ti_{4.95}Nb_{0.05}O_{12}$ discharge to **a** 0 V and **b** 1 V at the current density of 35 mA g^{-1}; Cycling performance and columbic efficiency of $Li_4Ti_5O_{12}$ and $Li_4Ti_{4.95}Nb_{0.05}O_{12}$ discharged to **c** 0 V and **d** 1 V at the current density of 35 mA g^{-1}

our previous work, we have validated that the Nb ions have been successfully incorporated into the lattice structure of $Li_4Ti_5O_{12}$ [32]. As a result, the lattice constant is slightly enlarged, which is beneficial for fast lithium-ion transfer without lattice stability damaged.

The first, second, and third discharge–charge curves of $Li_4Ti_5O_{12}$ discharged to 0 V at the current density of 350, 875, and 1,750 mA g^{-1}, and discharged to 1 V at the current density of 1,750 mA g^{-1} are shown in Fig. 2. The initial discharge capacity of $Li_4Ti_5O_{12}$ decreases with the current densities increasing. When the current density is increased from 350 to 1,750 mA g^{-1}, the second and third discharge plateaus become slowly inconspicuous. However, $Li_4Ti_5O_{12}$ discharged to 1 V at the current density of 1,750 mA g^{-1} shows an obvious discharge plateau. In order to explain the different discharge plateau characteristic for $Li_4Ti_5O_{12}$ discharged to 1 and 0 V at the current density of 1,750 mA g^{-1}, a sketch map of lithium-ion insertion and extraction for $Li_4Ti_5O_{12}$ discharged to 1 V and 0 V is proposed in Fig. 3. For discharging down to 1 V at the high current density, the center of $Li_4Ti_5O_{12}$ particle has not totally transformed to $Li_7Ti_5O_{12}$ (Fig. 3a). But when being charged to 2.5 V, the original $Li_4Ti_5O_{12}$ can be resumed, because lithium extraction is easier kinetically than lithium insertion in $Li_4Ti_5O_{12}$ due to the repulsive interactions between neighboring lithium ions during lithium insertion [33]. However, when discharged to 0 V, $Li_4Ti_5O_{12}$ firstly transforms to $Li_7Ti_5O_{12}$ and further to $Li_{8.5}Ti_5O_{12}$ [34]. Usually the former process was described by a core-shell model, corresponding to a two-phase transition process, while in the latter process a single-phase transition of spinel/rock-salt occurred [35–38]. When fast lithium insertion and extraction are enforced at a high current rate, as shown in Fig. 3b, the two-phase conversion from $Li_4Ti_5O_{12}$ to $Li_7Ti_5O_{12}$ cannot be completely carried out in a limited time due to the

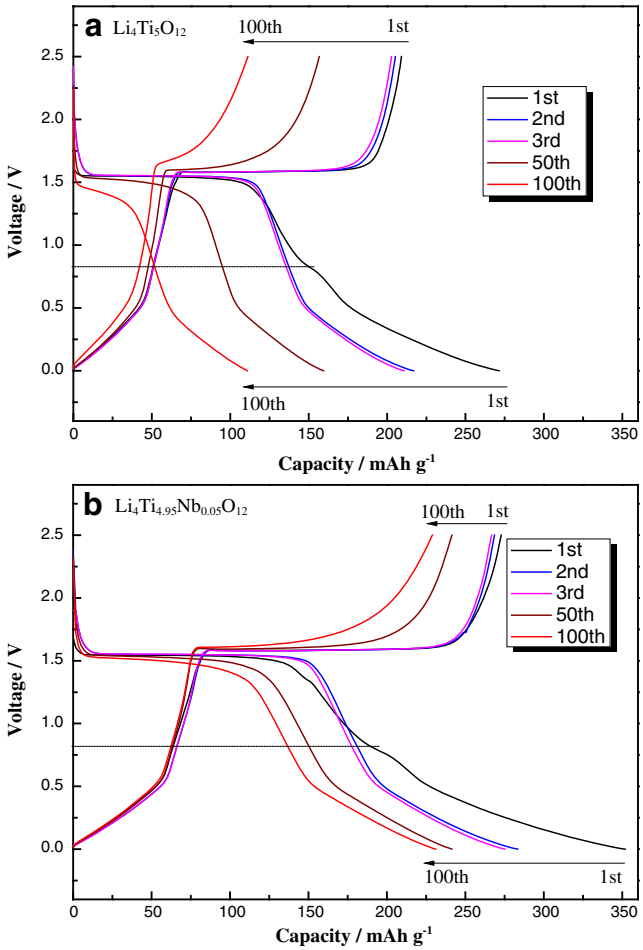

Fig. 5 The 1st, 2nd, 3rd, 50th, and 100th discharge–charge curves of **a** $Li_4Ti_5O_{12}$ and **b** $Li_4Ti_{4.95}Nb_{0.05}O_{12}$ discharged to 0 V at the current density of 35 mA g^{-1}

intrinsical poor conductivity of this material. Probably, a $Li_4Ti_5O_{12}$ core exists in the $Li_7Ti_5O_{12}$, and in the process of the single-phase conversion ($Li_7Ti_5O_{12} \rightarrow Li_{8.5}Ti_5O_{12}$), a transition phase of $Li_{4+\delta}Ti_5O_{12}$ could form around the core. During the lithium extraction, the original $Li_4Ti_5O_{12}$ cannot be retrieved completely, and $Li_{4+\delta}Ti_5O_{12}$ could exist inevitably. The higher current rate for lithium insertion/extraction can result in the more $Li_{4+\delta}Ti_5O_{12}$. In the sequent cycles, the existence of $Li_{4+\delta}Ti_5O_{12}$ is also the possible reason for the deformation of a flat discharge plateau. Based on the same mechanism (Fig. 3), $Li_{4+\delta}Ti_5O_{12}$ becomes $Li_{4+\delta'}Ti_5O_{12}$ ($\delta' > \delta$), so the capacity declines. Moreover, solid electrolyte interphase (SEI) film is formed with high impedance as the reduction of electrolyte at the low potential. So $Li_4Ti_5O_{12}$ exhibits an obvious capacity loss when discharged to 0 V, especially at the high current density. This conclusion also can be deduced from Shu's work [29].

The obvious capacity loss of $Li_4Ti_5O_{12}$ when discharged to 0 V mentioned above can be improved by doping Nb. The initial discharge–charge curves of $Li_4Ti_5O_{12}$ and $Li_4Ti_{4.95}Nb_{0.05}O_{12}$ electrodes down to 0 V and 1 V are shown in Fig. 4a and b. When cycled between 2.5 and 0 V, $Li_4Ti_{4.95}Nb_{0.05}O_{12}$ presents an initial discharge capacity of 351.9 mAh g^{-1} and a reversible charge capacity of 272.8 mAh g^{-1}, while $Li_4Ti_5O_{12}$ only has a discharge capacity of 271.5 mAh g^{-1} and a reversible capacity of 209.2 mAh g^{-1}. If all Ti^{4+} ions are reduced to Ti^{3+} ions, the theoretical capacity of $Li_4Ti_5O_{12}$ will be 293 mAh g^{-1} [29]. In fact, on the basis of Zhong's [34] report, $Li_4Ti_5O_{12}$ is transferred into $Li_{8.5}Ti_5O_{12}$ (not $Li_9Ti_5O_{12}$, corresponding to full reduction from Ti^{4+} to Ti^{3+}) when discharged to 0 V, which is corresponding to a reversible capacity of about 262 mAh g^{-1}. During the initial discharge (lithium insertion), the high discharge capacity is related to the deep lithium insertion (the highest value: 262 mAh g^{-1}) into the active material ($Li_4Ti_5O_{12}$ or Nb-doped $Li_4Ti_5O_{12}$), some side reactions for SEI formation and lithium adsorption in the carbon black [39]. The higher reversible charge capacity of Nb-doped $Li_4Ti_5O_{12}$ is mainly attributed to the lithium extraction from the active material (close to the theoretical value: 262 mAh g^{-1}) and lithium desorption from the carbon black (about 10~20 mAh g^{-1}). Figure 4c and d show the cycling performances and columbic efficiencies of $Li_4Ti_5O_{12}$ and $Li_4Ti_{4.95}Nb_{0.05}O_{12}$ at the current of 35 mA g^{-1} down to 0 V and 1 V. When the cells are discharged to 1 V at the same current density, the 100th discharge capacity of $Li_4Ti_{4.95}Nb_{0.05}O_{12}$ is 157.4 mAh g^{-1}, but the corresponding value of $Li_4Ti_5O_{12}$ is 135.7 mAh g^{-1}. The improvement in capacity can be attributed to Nb^{5+} doped into the lattice of the $Li_4Ti_5O_{12}$, as we discussed in our previous paper [32]. The 100th discharge capacity of $Li_4Ti_{4.95}Nb_{0.05}O_{12}$ down to 0 V is 231.2 mAh g^{-1} while the capacity of $Li_4Ti_5O_{12}$ is only 111.1 mAh g^{-1}. The specific capacity retentions of $Li_4Ti_{4.95}Nb_{0.05}O_{12}$ and $Li_4Ti_5O_{12}$ are 81.6% and 51.2% except the initial discharge. Obviously, when discharged to 0 V, the two spinel materials have a big gap on the capacity and cycling performance. The improvement in capacity can also be attributed to Nb^{5+} doped into the lattice of the $Li_4Ti_5O_{12}$. Compared with $Li_4Ti_5O_{12}$, the lattice constant of the $Li_4Ti_{4.95}Nb_{0.05}O_{12}$ is enlarged, which results in the broader path for lithium insertion and extraction [40, 41]. For the enhanced cycling stability of Nb-doped $Li_4Ti_5O_{12}$, the main reasons are the enlarged lattice constant and improvement on the conductivity due to the introduction of Nb^{5+} in the lattice, which are helpful for suppressing the formation of $Li_{4+\delta}Ti_5O_{12}$.

The 1st, 2nd, 3rd, 50th, and 100th discharge–charge curves of $Li_4Ti_5O_{12}$ and $Li_4Ti_{4.95}Nb_{0.05}O_{12}$ discharged to 0 V at the current density of 35 mA g^{-1} are plotted in Fig. 5. It can be seen that both $Li_4Ti_5O_{12}$ and $Li_4Ti_{4.95}Nb_{0.05}O_{12}$

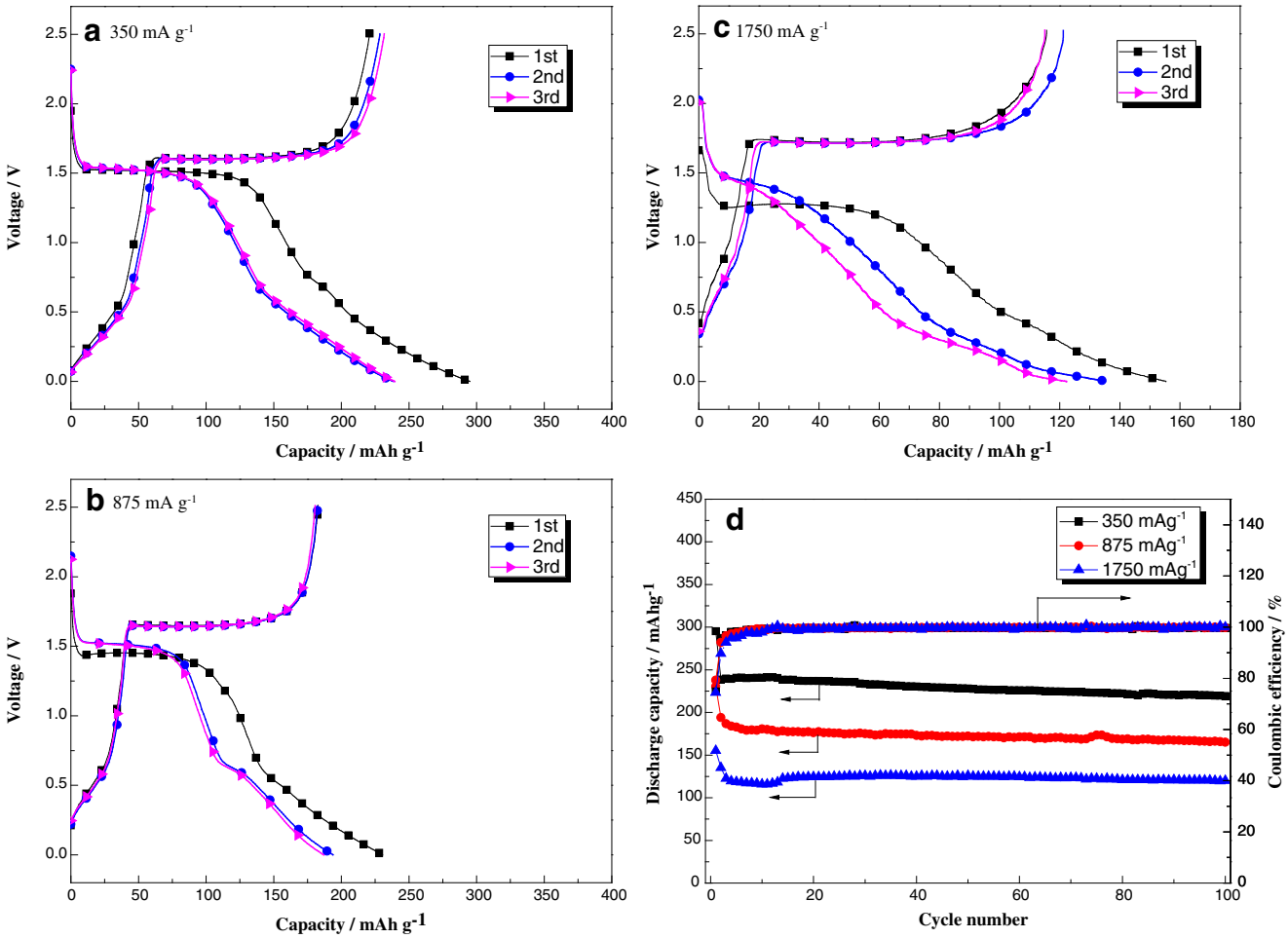

Fig. 6 The first, second, and third discharge–charge curves (**a**), (**b**), and (**c**); cycling performance and columbic efficiency (**d**) of $Li_4Ti_{4.95}Nb_{0.05}O_{12}$ discharged to 0 V at the current density of 350, 875, and 1,750 mA g^{-1}

show a loss of the 1.55 V plateau with increasing the cycling number. However, $Li_4Ti_{4.95}Nb_{0.05}O_{12}$ shows a much slower plateau capacity loss than $Li_4Ti_5O_{12}$ with increasing the cycling number, which indicates that Nb-doping is beneficial to the electrochemical stability of $Li_4Ti_5O_{12}$ during the electrochemical process for discharging to 0 V. However, there is an obvious irreversible capacity between initial discharge and charge processes. It mainly occurs in the voltage range of 0.75~0 V for the formation of SEI film with high impedance [39].

The first, second, and third discharge–charge curves, cycling performance and columbic efficiencies of $Li_4Ti_{4.95}Nb_{0.05}O_{12}$ discharge to 0 V at the current density of 350 mA g^{-1}, 875 mA g^{-1} and 1,750 mA g^{-1} are shown in Fig. 6. The discharge capacity of $Li_4Ti_{4.95}Nb_{0.05}O_{12}$ is 219.1 mAh g^{-1} at the current density of 350 mA g^{-1} after 100 cycles. When the higher current densities are adopted, $Li_4Ti_{4.95}Nb_{0.05}O_{12}$ still keeps excellent cycling performance and high columbic efficiency (~100%). And, it retains a discharge capacity of 120.2 mAh g^{-1} after 100 cycles even at the current density of 1,750 mA g^{-1}. The excellent cycling performance of the $Li_4Ti_{4.95}Nb_{0.05}O_{12}$ at the high current densities is mainly related to the enlargement of the lattice constant and the improvement of electronic conductivity [32].

Conclusion

$Li_4Ti_{4.95}Nb_{0.05}O_{12}$ powder has been successfully synthesized by a sol–gel method with citric acid as a chelating agent. XRD patterns show that $Li_4Ti_{4.95}Nb_{0.05}O_{12}$ has good crystallinity. The electrochemical performance of $Li_4Ti_{4.95}Nb_{0.05}O_{12}$ discharged to 0 V has been investigated. It is found that $Li_4Ti_{4.95}Nb_{0.05}O_{12}$ has a higher specific capacity and better cycling stability than $Li_4Ti_5O_{12}$. $Li_4Ti_{4.95}Nb_{0.05}O_{12}$ exhibits a capacity of 231.2 mAh g^{-1} at the current of 35 mA g^{-1} even after 100 cycles. All lines of evidence demonstrate that Nb-doping is beneficial to the electrochemical stability of $Li_4Ti_5O_{12}$ discharged to 0 V.

Acknowledgments This work was supported by National Science Foundation of China (grant no. 21006033), Program for New Century Excellent Talents in Chinese Ministry of Education (No. NECT-07-0307) and the Fundamental Research Funds for the Central Universities, SCUT (2009220038).

References

1. Kanamura K, Naito H, Takehara Z (1997) Chem Lett 1:45–46
2. Peramunage D, Abraham KM (1998) J Electrochem Soc 145:2609–2615
3. Zaghib K, Simoneau M, Armand M, Gauthier M (1999) J Power Sources 81–82:300–305
4. Tarascon JM, Armand M (2001) Nature 414:359–367
5. Ariyoshi K, Yamato R, Ohzuku T (2005) Electrochim Acta 51:1125–1129
6. Ohzuku T, Ueda A, Yamamoto N (1995) J Electrochem Soc 142:1431–1435
7. Tang YF, Yang L, Qiu Z, Huang JS (2008) Electrochem Commun 10:1513–1516
8. Jiang CH, Zhou Y, Honma I, Kudo T, Zhou HS (2007) J Power Sources 166:514–518
9. Hao YJ, Lai QY, Liu DQ, Xu Z, Ji XY (2005) Mater Chem Phys 94:382–387
10. Guerfi A, Charest P, Kinoshita K, Perrier M, Zaghib K (2004) J Power Sources 126:163–168
11. Bruce PG, Scrosati B, Tarascon J-M (2008) Angew Chem Int Ed 47:2930–2946
12. Wang D, Xu HY, Gu M, Chen CH (2009) Electrochem Commun 11:50–53
13. Liu P, Sherman E, Verbrugge M (2010) J Solid State Electrochem 14:585–591
14. Zhao YM, Liu GQ, Liu L, Jiang ZY (2009) J Solid State Electrochem 13:705–711
15. Huang SH, Wen ZY, Zhang JC, Yang XL (2007) Electrochim Acta 52:3704–3708
16. Huang SH, Wen ZY, Lin B, Han JD, Xu XG (2008) J Alloy Compd 457:400–403
17. Liu H, Feng Y, Wang K, Xie JY (2008) J Phys Chem Solids 69:2037–2040
18. Yu HY, Zhang XF, Jalbout AF, Yan XD, Pan XM, Xie HM, Wang RS (2008) Electrochim Acta 53:4200–4204
19. Dominko R, Gaberscek M, Bele M, Mihailovic D, Jamnik J (2007) J Eur Ceram Soc 27:909–913
20. Huang JJ, Jiang ZY (2008) Electrochim Acta 53:7756–7759
21. Mukai K, Ariyoshi K, Ohzuku T (2005) J Power Sources 146:213–216
22. Huang SH, Wen ZY, Zhu XJ, Lin ZX (2007) J Power Sources 165:408–412
23. Zhao HL, Li Y, Zhu ZM, Lin J, Tian ZH, Wang RL (2008) Electrochim Acta 53:7079–7083
24. Yi TF, Shu J, Zhu YR, Zhu XD, Yue CB, Zhou AN, Zhu RS (2009) Electrochim Acta 54:7464–7470
25. Wolfenstine J, Allen JL (2008) J Power Sources 180:582–585
26. Kubiak P, Garcia A, Womes M, Aldon L, Olivier-Fourcade J, Lippens PE, Jumas JC (2003) J Power Sources 119–121:626–630
27. Ganesan M (2008) Ionics 14:395–401
28. Ge H, Li N, Li DY, Dai CS, Wang DL (2009) J Phys Chem C 113:6324–6326
29. Shu J (2009) J Solid State Electrochem 13:1535–1539
30. Borghols WJH, Wagemaker M, Lafont U, Kelder EM, Mulder FM (2009) J Am Chem Soc 131:17786–17792
31. Xiang HF, Zhang X, Jin QY, Zhang CP, Chen CH, Ge XW (2008) J Power Sources 183:355–360
32. Tian BB, Xiang HF, Zhang L, Li Z, Wang HH (2010) Electrochim Acta 55:5453–5458
33. Jung KN, Pyun SI, Kim SW (2003) J Power Sources 119–121:637–643
34. Zhong ZY, Ouyang CY, Shi SQ, Lei MS (2008) Chemphyschem 9:2104–2108
35. Scharner S, Weppner W, Schmid-Beurmann P (1999) J Electrochem Soc 146:857–861
36. Ma J, Wang C, Wroblewski S (2007) J Power Sources 164:849–856
37. Lu W, Belhaeouak I, Liu J, Amine K (2007) J Electrochem Soc 154:A114–A118
38. Takami N, Inagaki H, Kishi T, Harada Y, Fujita Y, Hoshina K (2009) J Electrochem Soc 156:A128–A132
39. Yao XL, Xie S, Nian HQ, Chen CH (2008) J Alloy Compd 465:375–379
40. Huang YD, Jiang RR, Bao SJ, Dong ZF, Cao YL, Jia DZ, Guo ZP (2009) J Solid State Electrochem 13:799–805
41. Yi TF, Shu J, Zhu YR, Zhu XD, Zhu RS, Zhou AN (2010) J Power Sources 195:285–288